Library Progress International
Vol.44 No.3, Jul-Dec 2024: P. 23098-23110

Print version ISSN 0970 1052
Online version ISSN 2320 317X

Original Article

Available online at www.bpasjournals.com

Study of optical UV absorption and optical band gap determination of polyaniline with CuO

[1*]Ramabai N, [2,] Dr. Basavaraj Sannakki

[1,] Department of Physics, SSA GFGC (A), BALLARI-583101, Karnataka State, India.
[and 2] Department of Physics, Gulbarga University, KALABURAGI-585106, Karnataka State, India.
Corresponding Author: ramabaissagfgc@gmail.com

How to cite this article: Ramabai N, Basavaraj Sannakki (2024). Study of optical UV absorption and optical band gap determination of polyaniline with CuO. *Library Progress International,* 44(3), 23098-23110

Abstract:
The optical characteristics and optical band gap of polyaniline (PANI) composites with copper oxide (CuO) are the main subjects of the investigation. CuO is a copper oxide with semiconducting qualities, while polyaniline is a conductive polymer with potential uses in electronics, sensors, and optoelectronic devices. It is anticipated that the combination of these materials will result in composite structures with improved optical qualities. In order to investigate the optical absorption behaviour of PANI/CuO composites in the UV region, UV-Visible (UV-Vis) spectroscopy was used to synthesise the materials using chemical oxidative polymerisation. The PANI/CuO composite's optical absorption spectra showed notable UV absorption, indicating the material's potential for use in optoelectronic applications. Tauc's graphic, which demonstrated a straightforward band gap transition, was used to calculate the optical band gap from the absorption data. According to the research, adding CuO changed polyaniline's band gap, improving its electrical characteristics and increasing the material's suitability for photovoltaic and photocatalytic uses. The addition of CuO greatly reduces the optical band gap of PANI, a property that may be tailored for certain applications by altering the CuO level in the composite, according to the findings. This research highlights the promise of PANI/CuO composites in improving materials design where control over optical characteristics and band gap is essential, such as in energy harvesting, UV detection, and optoelectronics.
Keywords: *Polyaniline, CUO, UV Absorption, Band Gap*

1. Introduction

Conducting polymer nanocomposites are a visually appealing material with distinctive properties that make them suitable for a broad variety of potential applications, involving light-emitting diodes (LEDs), solid-state batteries, and storage devices like supercapacitors. Notwithstanding its popularity for stability in the environment, comparatively good electrical conductivity, large surface to volume ratios, efficiency of production, and convenience of processing in a basic testing facility, PANI is one of the conducting polymers that has been thoroughly studied. PANI is a redox-active catalyst that increases the value of energy devices. PANI Emeraldine Salt effectively protects metal oxide from dissolving in acidic electrolytes.

Despite polymers have been used in the electrical and electronics industries as fundamental materials for electrical capacitors or as thermal or electrical insulation, their usage in solar cells and diodes and other electronic applications has increased due to the the likelihood of enhancing their electrical conductivity through deformation or the addition of metallic materials like copper or silver. Due to their many uses in the medical, engineering, and industrial fields, as well as their affordability when contrasted with inorganic materials, polymeric materials have gained a lot of notoriety recently. This is because polymers have special characteristics that make them easy to handle in an industrial setting. These properties include an array of optical, mechanical, and electrical attributes that can be regulated through a variety of chemical and physical treatments.

Because of the special electrical, optical, mechanical, magnetic, and chemical capabilities of metal nanoparticles, researchers have been concentrating on their synthesis in recent years. Uniformity, phase continuity, domain sizes, and molecule mixing at phase boundaries are significant chemistry-related elements that play a direct role in the advancement of these systems and directly impact their optical, physical, and mechanical properties [20]. Recent years have seen a important rise in interest in nanocrystalline semiconductor particles because of their specific electrical and optical characteristics, and also their enormous surface-to-volume ratio when compared to bulk materials [11]. One type of transition metal oxide is CuO [12].

CuO compounds are widely recognised technological materials with applications in solar energy, electronics, gas sensing, magnetic media, optical devices, batteries, and catalysts. They are also used to construct junction devices like p-n diodes and for photoconductive, photothermal processes [13].

CuO-NPs, or CuO nanoparticles, are semiconducting materials with strong absorption capabilities and direct band gaps. Numerous fields have seen their application, including as solar cells [3], magnetic storage medium [1], photodetectors [2], field emissions, and nanofluid. Biosensors [4], gas sensors, super-capacitors, photocatalysis, antiviral and antibacterial qualities, and photocatalysis are more applications. CuO-NPs have the potential to weaken and undermine the integrity of the virus's genome. It has been demonstrated that CuO-NPs can pierce the virus's membrane [5]. By impregnating N95 masks with CuO-NPs was created possible, which improved mask's antiviral activity five times over.

Because of their special physical and chemical characteristics, conducting polymers have a wide range of applications, involving organic field-impact transistors, plastic solar cells, sensors, rechargeable batteries, and compounds. Polymers are a type of materials that are semi-crystalline, amorphous, heat-sensitive, and electrically insulating. Inorganic elements can be added to polymers to change their electrical characteristics. Because of their fascinating features arising from their huge surface area and nanosized size, nanoscale particles are interesting as fillers. The electric and dielectric characteristics of the host polymers may be enhanced by the doping of nanoscale components.

PANI, one of the many conducting polymers, has drawn a lot of interest due to its easy synthesis, environmental stability, intriguing redox nature, and adjustable electro-optical features. Inorganic fillers could be added to conducting polymers to change their electrical characteristics. The XRD, SEM, FTIR, and UV-visible spectroscopy are used in this work to characterise chemically synthesised PANI in the form of emeraldine powder. In-depth research is done on the obtained samples' dielectric characteristics. To the best of our knowledge, the current work completely reports the structural and dielectric properties of PANI/CuO at higher frequencies. Measurements of dielectric as a matter of frequency and temperature are made.

Due to its special qualities—such as excellent conductivity, thermal stability, and environmental stability—PANI has been the subject of extensive research. The kind and size of the ions in the polymer backbone of this material, which has a doping protonic oxidation

level, influence the electronics range from insulators to conductors. Pani possesses half-oxidized emeraldine base, fully oxidised base (PB), and entirely basic reduced form leucoemeraldine base. LEB, identified by electronic transitions between the conduction and valence bands, exhibits the lowest energy absorption in the 320 nanometer range. In order to contribute locally to electronic transitions π-π* content transfer among the ring and the imine unit—phenylamine neighbouring quinoid added intramolecular charge transfer exciton—for EB absorption, an energy range of 600 nm is needed.

Emerald salt plays the job of enhancing electrical conductivity as a result of this quality. Peierls gap transition is used to characterise different types of energy absorption at 320 nanometer and 530 nanometer PB. The most popular techniques for creating nanomaterials can be roughly divided into two categories: bottom-up techniques (chemical and bio-assisted) and top-down techniques (physical techniques). Nevertheless, the green synthesis approach, which is gaining popularity due to its affordability and convenience of use, can lessen the limits of these methods.

In addition, synthetic polymer polyvinyl alcohol (PVA) has attracted a lot of interest lately because of its unique chemical and physical characteristics. This water-soluble polymer is both environmentally benign and nontoxic. In addition, it has a strong dielectric strength, is elastic and ductile yet rigid, and is resistant to oil, grease, and solvents. It also performs admirably as an oxygen and odour barrier [6]. In addition, PVA is used in the manufacturing of ophthalmic lubricants, cosmetics, pharmacological aids, surface coatings, and artificial sponges, among other goods.

When creating novel materials for solar cells, managing the band gap is crucial. In order to create new materials with the most crossover among their absorption and solar emission spectra, researchers attempted to develop and synthesise them [7]. These two characteristics of organic materials will be controlled by the inclusion of nano-inorganic compounds like CuO-NPs. Both measure the final solar conversion efficiency and are depending on band structure. To close the band gap and improve solar energy harvesting, it is crucial to investigate the optical and electrical characteristics of CuO-PVA NCs[8].

Because of its comparatively strong band gap, PVA minimises light harvesting and restricts the absorption of visible light. As such, its application as an active layer in organic solar cells is improper. A semiconducting material's band gap and optical absorption play important roles in determining whether or not to employ it as an active layer in solar cells. In order to overcome the shortcomings of their counterparts, unique nanomaterials with improved physical and chemical attributes could be created by combining the qualities of inorganic CuO-NPs and organic PVA [9]. According to reports, inorganic-organic nanocomposites have the potential to be used in gas sensors, solar cells, because they improve the band gap and optical absorption [10].

When evaluating the optical behaviour of CuO nanoparticles, UV-vis and photoluminescence techniques are primarily used to examine electronic transitions in semiconductors. There aren't many publications on the absorption and band gap study of CuO nanoparticles that use UV–vis analysis. Nevertheless, nothing is known about CuO nanoparticles' optical characteristics.

2. Literature Review

Using GCD and CV methods, the electrochemical effectiveness of PANI/CuO NCs (PCN) for energy storage device technologies has been investigated. As the concentration of CuO nanoparticles increases, the surface morphology exhibits significant variations from granular shape to fine rodlike architecture [14]. PANI and PCN2 nanocomposite absorption peaks were seen to redshift (move towards higher wavelengths) and to decrease in optical band gap (Eg) from 2.86 eV to 2.59 eV, correspondingly. According to the aforementioned findings, the PCN

is crucial in improving long-lasting cyclic stability for applications involving supercapacitors. Using the spin coating method, thin films of semiconducting PANi nanofibers reinforced with CuO nanoparticles (NPs) were created on a glass substrate. By using monomer aniline in the existence of (NH4)2S2O8 as an oxidant and oxidative polymerisation at 0 °C, PANi has been created. The sol-gel approach was used to create the CuO nanoparticles [15]. X-ray diffraction, SEM, FTIR spectroscopy, UV–vis spectroscopy, two probe resistivity measuring technologies, and thermo-emf measurement were used to characterise and analyse the physical attributes of NCs films. According to structural studies, the PANi–CuO hybrid nanocomposite does not disrupt the crystal structure of CuO. A examination of surface morphology reveals that CuO nanoparticles are uniformly distributed throughout the PANi matrix. Studies using FTIR and UV-Visible technology verify that PANI is present in the composites in the emeraldine base form and propose that CuO may have been added to the polymer. According to two probe electrical resistivity studies of nanocomposites (NCs) film, PANi's resistivity rises as CuO NP content does.

Utilising the chemical oxidative polymerisation technique, polyaniline/CuO composites are created at various weight percentages [16]. The composites have been synthesised with different compositions (10, 15, and 20 weight percent) of CuO in PANI. The PANI and CuO doped PANI composite have been confirmed to be synthesised using PL (photoluminescence spectroscopy) approaches, FT-IR, UV-vis, and XRD (X-ray diffraction) chemical characterisation methods. These composites' surface morphology is examined using a SEM.

The current study used a straightforward solution cast process to create pure films of nanocomposite including copper oxide (CuO) and polyvinyl alcohol (PVA). A thorough analysis was conducted on the produced films' optical and structural characteristics. CuO NPs at various weight percentages (0.1–0.4 wt%) were produced and added to the PVA film. The profiles obtained from XRD reveal the existence of CuO nanoparticles (NPs) in PVA film. The CuO NPs were integrated into the PVA host matrix, according to the XRD data, and there were no extra impurity peaks [17]. The XRD data validate that the produced CuO NPs are in the monoclinic phase. The peak that was noticed at $2\theta = 19.4°$ is indicative of the semi-crystalline PVA polymer production. The prepared NPs were found to have an average crystallite size of approximately 0.52 nm. Plots using FTIR verified the presence of vibrational bands in the produced films. Raman spectra were used to further explore the NPs' presence in the films. The UV-visible optical absorption spectra were obtained in order to assess the produced films' band gap values. It was discovered that the band gap value for pure PVA is 5.35 eV, and that it minimises as the concentration of CuO NPs increases because the electrical structure of the pure PVA changes.

CuO and PANI were combined to create a nanocomposite material. The produced nanocomposites were examined using electrochemical, AFM, FTIR, UV-Vis, and SEM analyses. FTIR spectrum investigations identified the polymer and metal oxide present in the nanocomposites [18]. AFM and SEM were used to characterise the surface morphology. Cyclic voltammetry was used to establish the optical properties, whereas UV-visible spectroscopy was used to determine the electrochemical parameters. These analyses showed that Polyaniline/CuO was a novel semiconductor photoelectric material, and Polyaniline/CuO-prepared solar cells had good performance.

Using an in-situ chemical reaction technique, a composite of PANI and lithium chloride (LiClO4) was created with CuO nanoparticles submerged in it. FT-IR, FESEM, and UV-Vis spectroscopy [19] were used to characterise the composite in order to verify the development of chemical interactions, changes in surface morphology, and changes in optical characteristics. The optical investigation shows that the stretching of the benzenoid ring causes the π-π^* electron transition, which results in a red shift in wavelength from 310 nanometer to 375 nanometer. For PL to PLC composites, the direct optical band gap exhibits a minimising trend

of 2.62 eV and 2.56 eV, correspondingly. These findings imply that composite materials based on PANI are appropriate for use in electrochromic devices, solid state batteries, and optoelectronic displays.

Through the use of chemical synthesis, pure hybrid composites are created. Studies on the samples' morphology, electrical properties, optical properties, and structure were conducted. When hybrid composites are compared to pure PANI, their FT-IR spectra are shown to be pushed towards higher wave numbers [21]. The XRD spectrum verifies the synthesis of hybrid composites.

It has been noted that hybrid composites produced at varying weight percentages of APS exhibit morphological changes. According to the SEM data, PANI samples have a smooth, spherical morphology, while hybrid composites have an aggregated morphology. The growth of DBSA and evenly distributed CuO-doped composite nanoparticles in the polymer matrix are visible in the TEM morphology.

In comparison to pure PANI, the PANI/CuO composites show comparatively high photoluminescence intensity in the violet and green-yellow regions of the visible spectrum as well as good electrical conductivity. Due to the creation of new conduction routes, the composites exhibit a semiconducting character and their conductivity diminishes as the APS concentration increases.

3. Research Methodology

Prior to usage, 99.9% of the aniline monomer was distilled. CuO, ammonium persulphate (NH4)2S2O8, and hydrochloric acid, H2SO4, and potassium chloride were all acquired from Sigma-Aldrich. A solution of 0.2 M aniline was made in 1 M HCl and a separate solution of 0.2 M ammonium per sulphate (2 g) in 1 M HCl was agitated. The APS solution was gradually added to the aniline, and an ice bath was used to keep the freezing temperature among 0 and 3 °C. The sample was electrochemically deposited on a carbon electrode using the CHI-660 Electrochemical Workstation apparatus, which allowed for 900 s of deposition duration at a voltage of 2 V.

The end product, PANI emaraldine salt (ES), left behind residue that was dark green in hue. PANI/CuO nanocomposite was treated in a similar way at concentrations of 0.05, 0.2, and 2 g CuO NC; these were coded as PCN0.05, PCN0.2, and PCN2, correspondingly. As seen in the schematic picture above, the PANI polymerisation occurs as a result of a chemical reaction among the APS in the aqueous phase and the aniline monomers in the organic phase. Platinum and silver served as reference and counter electrodes, while carbon served as the working electrode.

The resulting PANI residue was filtered using whatman paper, repeatedly cleaned with distilled water, and baked for roughly 24 hours at 60 °C. In order to turn the sample into powder, it was lastly ground using a pestle and mortar. The PCN NCs electrode was created on a stainless steel surface measuring 1 x 1.5 cm2. The paste was made using a doctor blade and a ratio of PCN to PVDF to carbon in NMP solvent. The electrode was then dried in a vacuum oven at 40 °C for approximately 24 hours. Lastly, the cyclic effectiveness of PANI/CuO NCs were investigated using the CV and GCD.

Optical measurements of PANI nanofibers in the 350–700 nanometer wavelength range were performed at room temperature using a Shimadzu UV–VIS scanning spectrophotometer. Absorption spectra on a clean glass substrate after nanofiber PANI was deposited. The optical constants, like the refractive index n and absorption coefficient α, were estimated from transmittance spectra using Swanepoel's envelope approach. The interference fringes of transmission data collected over the visible range were used to calculate the thickness of the PANI nanofiber layer on the substrate.

A FT-IR with a model Alpha Bruker spectrometer was used to study the chemical interaction in the 2400–500 cm1 spectral region. Sigma Zeiss field emission SEM was used to evaluate the surface morphology. The structural alteration is investigated using a benchtop XRD, a RigaKu 600 Miniflex. The TEM is used to analyse the size of the particles, and this equipment operates at 200 keV with a point resolution of 0.23 nanometer and a lattice resolution of 0.14 nanometer.

Under a nitrogen flow rate of around 20 mL/min, the TGA, DTA, and DSC are investigated using TA instruments Q-600 heating from 30 to 700 °C at the heating rate of 10 °C/min. A computerised, integrated double beam Perkin-Elmer Lambda-35 UV-visible spectrophotometer operating in the wavelength range of 190–1100 nanometer was used to measure the optical absorbance (A). The dielectric property was measured using a room-temperature. A CHI-660E electrochemical workstation was used to monitor galvanostatic charging and discharging, CV, and EIS.

4. Results and Discussion

FT-IR spectroscopy is utilised to investigate the chemical interaction between PANI and PCN NC. The C-N and C-C ring stretching vibrations are attributed to the PANI's peak values at 1286 and 1561 cm−1, correspondingly. With an increase in CuO NC concentration, the band of interest at 878 cm−1 changes towards a higher wavenumber, which is associated with bending vibration of the C-H plane in PANI.

The peak seen at 2356 corresponds to FT-IR transmittance spectra of various CuO-doped nanocomposites. 2359 cm−1 aromatic and aliphatic stretching vibrations. The CuO NC exhibit increased wave numbers.

Table.3.1. Effect of Scan Rate on Maximum Current Density and Potential Range

Scan rate	Maximum current density	Potential range
100mV/s	~2.0 x 10^-5	-3.5 to 1.5
200mV/s	~2.1 x 10^-5	-3.5 to 1.5
300mV/s	~2.3 x 10^-5	-3.5 to 1.5
400mV/s	~2.6 x 10^-5	-3.5 to 1.5
500mV/s	~2.8 x 10^-5	-3.5 to 1.5

Table.3.2. DSC graph of nanocomposites.

Temperature (°C)	Heat Flow - PANI	Heat Flow - PCN0.05	Heat Flow - PCN0.2	Heat Flow - PCN2
100	~10	~8	~8	~8
135 (Peak)	~15	~13	~13	~12
145 (Peak)	~25	~22	~22	~22
200	~30	~27	~25	~27
400	~30	~35	~32	~45
500	~20	~25	~25	~30
600	~0	~-5	~0	~5
700	~45	~47	~50	~55
800	~-10	~-5	~-5	~-10

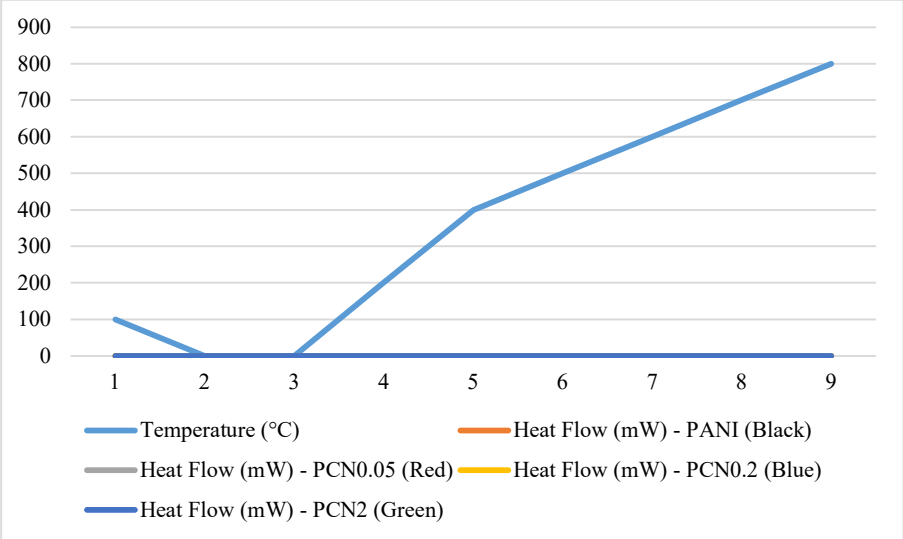

Fig.3.1. DSC graph of nanocomposites.

For the PCN 2 NC with the strongest concentration, the PANI picture displays a globular-like morphology with minimal porosity and a significant variation in morphology from globular to rod form architecture. Since the mobility of electrons in a rod-shaped structure is faster than on a rough surface of the sample, the conductivity is higher in the rod-like shape. The rod-shaped morphology seen in the PCN NC photograph amply illustrates the uniform dispersion of the NC in the PANI matrix. A rod's average radius ranges from 80 to 100 nm. These microstructure alterations could validate the impact of the nano composite within the polymer matrix.

It displays dense, gloomy areas that highlight PANI's conducting qualities. On the other hand, the PCN 0.2 image demonstrates more nanoparticles are present on the PANI and displays a dense, black zone caused by agglomerated nanoparticles. The black and white backgrounds in all of the TEM PCN nanocomposite photos indicate host polymer PANI, though the dark portion displays CuO nanocomposites. Particle sizes ranged from 30 to 80 nm on average. The dense, black area imbedded in the white background suggests that there are more metal ions present.

Table.3.3. TGA thermogram curves of PANI and PCN NCs.

Temperature	Weight% - PANI	Weight% - PCN0.05	Weight% - PCN0.2	Weight% - PCN2
100	~7.8	~7.2	~6.5	~5.7
200	~7.2	~6.5	~5.8	~5.0
300	~6.7	~6.2	~5.2	~4.7
400	~6.1	~5.8	~4.7	~4.2
500	~4.5	~4.2	~3.5	~3.2
600	~1.8	~1.5	~1.0	~0.7
700	~0.2	~0.1	~0.0	~0.0
800	~0.0	~0.0	~0.0	~0.0

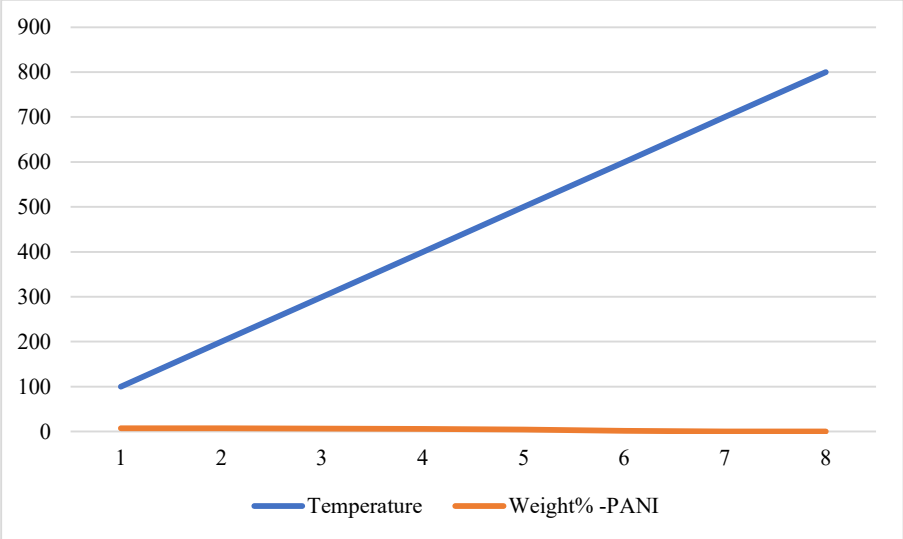

Fig.3.2. TGA Thermogram curves of PANI

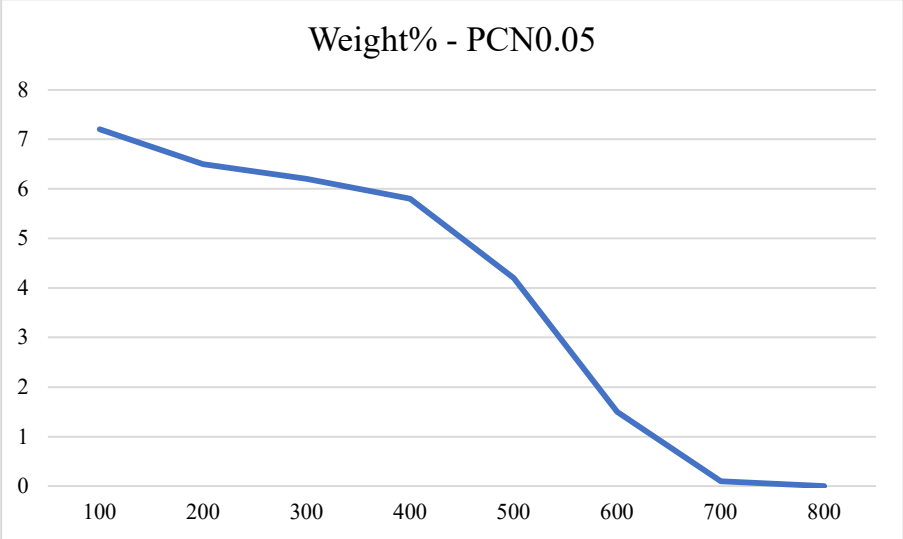

Fig.3.3. TGA Thermogram curves of PCN0.05

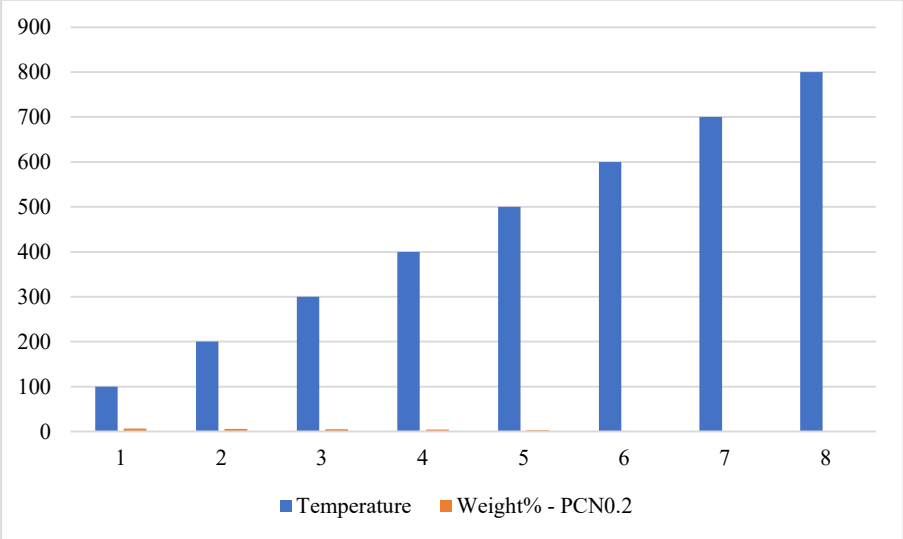

Fig.3.4. TGA Thermogram curves of PCN0.2

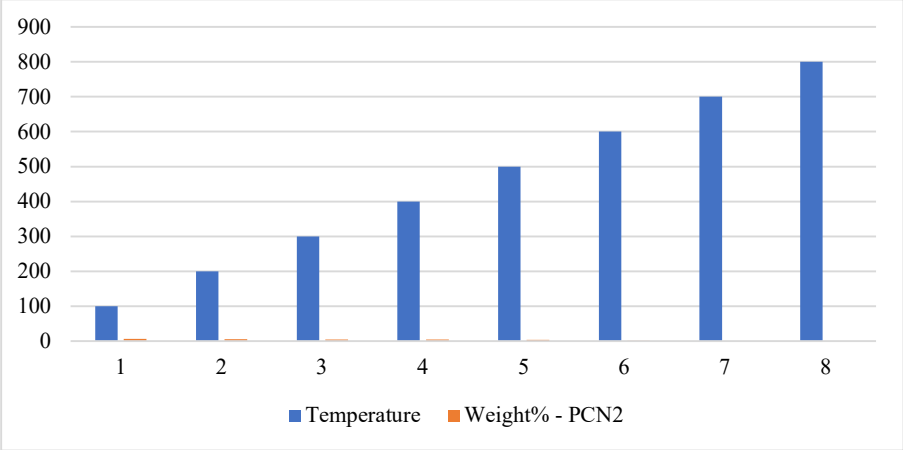

Fig.3.5. TGA Thermogram curves of PCN2

Table.3.4. DTA curve of PANI and PCN NCs.

Temperature	Deriv. Weight% - PANI	Deriv. Weight% - PCN0.05	Deriv. Weight% - PCN0.2	Deriv. Weight% - PCN2
100	~0.05	~0.05	~0.03	~0.02
200	~0.08	~0.07	~0.06	~0.05
300	~0.1	~0.1	~0.08	~0.08
400	~0.12	~0.13	~0.12	~0.11
500	~0.3	~0.35	~0.32	~0.4
600	~0.18	~0.15	~0.14	~0.12
700	~0.01	~0.01	~0.0	~0.0

Table.3.5. The absorption peaks

Samples	Absorption peaks	Optical band gaps
PANI	510	1.96
PCN 0.05	530	1.67
PCN 0.2	570	1.78

PCN 2	580	1.87

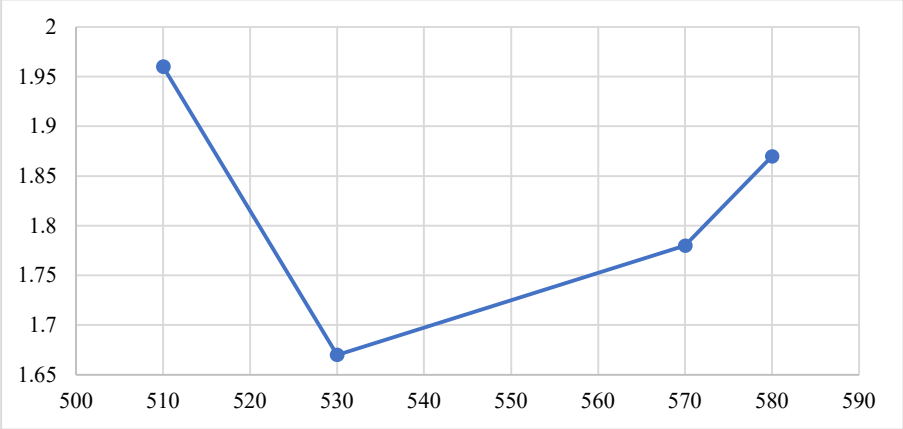

Fig.3.6. The absorption peaks

Table.3.6. The estimation of specific capacitance for various samples

Samples	Specific capacitance
PANI	176.89
PCN 0.05	257.09
PCN 0.2	287.56
PCN 2	1.678

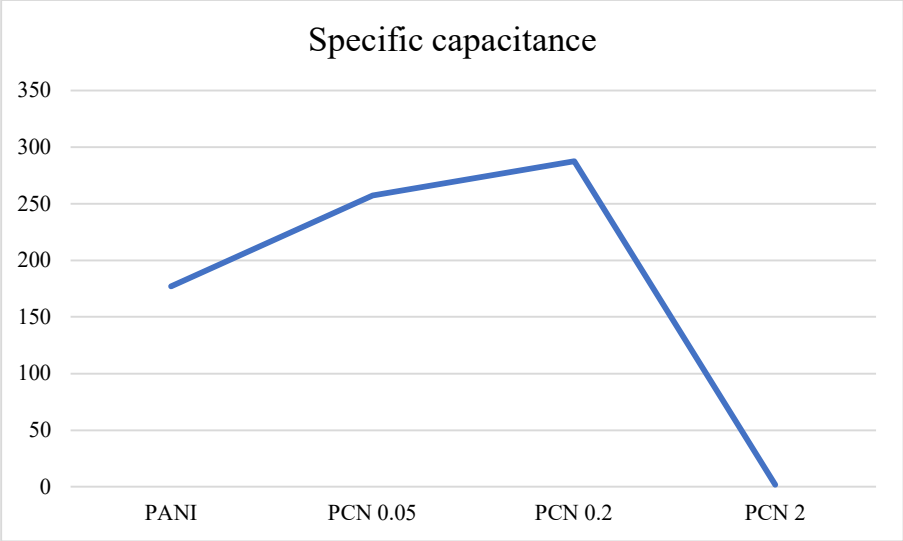

Fig.3.7. The estimation of specific capacitance for various samples

According to the TGA graph, thermal degradation happens in two stages. The first step occurs when moisture and water are present on the surface, and it happens between 78.91 and 102 °C, or around 14.03% of the total. The doping acid was lost during the second stage, which occurred between 110 and 650 °C, and the temperature at which the weight loss occurred changed. The degradation temperature decreases with rising nano CuO concentration in the PANI matrix. The substantially higher residual rate and lower degradation rate of PANI nanocomposites show their protective efficacy.

The thermal attributes of the electrochemically generated NCs give rise to the heat flow vs. temperature graphs. The broad endothermic shown in the DSC graphs at 140 °C corresponds to the monomer, water, and solvent molecules being removed. The melting point of PANI is determined to be 135 °C, while for PCN nanocomposites, it increases to 145 °C. These findings

demonstrate that the PCN nanocomposites outperform the PANI in terms of heat stability. The DTA curve exhibits exothermic peaks, reaching a maximum at 94.46 °C. This indicates that external water mole cules have been removed, and structural changes have been transferred to a temperature higher than that of PANI. The inclusion or influence of CuO nano concentration may be the cause of the improvement in thermal stability when compared to the host polymer PANI.

This study shows how the nano composite effect affects unsaturated bond variation and wavelength shifting. In the visible spectrum, the PANI absorption peak is seen at 625 nanometer. For the NCs, the absorption peak was seen at red shifts of 628, 632, and 656 nm, correspondingly. The absorption peak values and the chemical structural change from ben zenoid to quinoid excitonic transition have been linked to this shift.

The relationship between temperature and frequency and the ac conductivity varies. The disorder properties of the samples cause the ac conductivity to steadily grow with frequency.

PANI and PCN nanocomposites' galvanostatic charging-discharging (GCD) graphs are displayed. Because of the redox properties, these charging-discharging curves are maintained to be non-linear and quasi-symmetric in nature. Stability was attained due to the concentration of CuO nanoparticles.

As the concentration of CuO nanoparticles in the PANI increases, so does the specific capacitance value that is recorded. The PCN2 nanocomposite's greatest value at 0.05 A/g current density is 294 F/g. Maximum 4000 cycles are displayed when charging and discharging, indicating that the sample has excellent long-term cyclic stability and excellent storage stability. Electrochemical impedance spectroscopy is used to plot the Nyquist graph, which shows the electrical impedance of the imaginary part Z‡ vs the electrical impedance of the real part Z′. This technique is used to investigate the electrolyte ion transport and capacitance behaviour of the nano composites electrode over a wide frequency range.

Using a 1 M KCl electrolyte, the Nyquist plot of the PCN NC is performed in the frequency range of 0.1 to 100 kHz. The PANI and PCN electrodes' high-frequency and low-frequency regions both consist of a straight line with acceptable capacitive behaviour. The intrinsic resistance resulting from the electroactive material, the resistance arising from the electrolyte ions, and the resistance resulting from the contact among the interface can all be used to determine the charge transfer resistance interface.

5. Conclusion

Using the electrochemical deposition approach, PANI copper oxide nanocomposites (PCN) were effectively synthesised.

The outcomes point to an advancement in PANI/CuO NCs' thermal stability. A shift in the morphology from a granular to a nanorod-like framework verifies the appropriate dispersion. TEM images show that the particles are in the 30-80 nanometre range, and the presence of additional metal ions in the PCN is indicated by a thick, black region embedded on the white fibre background surface.The optical band gap indicates a decrease as the concentration of CuO nanocomposites grows.

The specific capacitance value of the pseudocapacitor, as indicated by the CV curve, is 424 F/g. The NC was fabricated with a proportion of 80:10:10. As a result, PANI/PCN nanocomposites become good candidates for energy storage device and supercapacitor applications. Chemical co-precipitation was the successful method used to create PAni-CuO nanocomposites.

The XRD data confirms the orthorhombic structure of all the produced nanocomposites, as per the reported results. The SEM micrograph makes the dispersion of CuO nanoparticles in the PAni matrix very evident, and the TEM data on the nanocomposite shows that its particle size

is approximately 7-8 nm, which is in good accord with the values found in the XRD data. The PAni-CuO nanocomposite exhibits metallic properties with an orthorhombic structure, as evidenced by the PL spectra, which also reveals certain electronic changes that have occurred in the composite. The IR and UV spectra highlight the involvement of the nano CuO particles. These characteristics make PAni-CuO nanocomposite composites potentially useful as shielding and absorbing materials at microwave frequencies.

PANI at different oxidation and protonation states has been studied using optical absorption. By progressively varying the acid strength of the buffer to which the polymer is exposed, the development of band structure correlating to the optical-absorption changes during the protonation of PANI at each distinct oxidation state is investigated. Using chemical and electrochemical methods, we have also evaluated the optical-absorption change at one fixed acid strength by gradually oxidising leucoemeraldine to emeraldine and finally to pernigraniline. The band structure alterations in connection with lattice structure interconversions during shifts among different oxidation and protonation states have been thoroughly studied.

References

1. Kumar, R. V., Diamant, Y., & Gedanken, A. (2000). Sonochemical synthesis and characterization of nanometer-size transition metal oxides from metal acetates. *Chemistry of Materials*, *12*(8), 2301-2305.
2. Wang, S. B., Hsiao, C. H., Chang, S. J., Lam, K. T., Wen, K. H., Hung, S. C., ... & Huang, B. R. (2011). A CuO nanowire infrared photodetector. *Sensors and Actuators A: Physical*, *171*(2), 207-211.
3. Santos-Cruz, J., Torres-Delgado, G., Castanedo-Perez, R., Jiménez-Sandoval, S., Jiménez-Sandoval, O., Zuniga-Romero, C. I., ... & Zelaya-Angel, O. (2005). Dependence of electrical and optical properties of sol–gel prepared undoped cadmium oxide thin films on annealing temperature. *Thin Solid Films*, *493*(1-2), 83-87.
4. Rahman, M. M., Ahammad, A. J., Jin, J. H., Ahn, S. J., & Lee, J. J. (2010). A comprehensive review of glucose biosensors based on nanostructured metal-oxides. *Sensors*, *10*(5), 4855-4886.
5. Fakhroueian, Z., & Esmaeilzadeh, P. (2020). The mirror strategy of nanoparticles against the coronavirus.
6. Abd El-Kader, K. M., & Orabi, A. S. (2002). Spectroscopic behavior of poly (vinyl alcohol) films with different molecular weights. *polymer Testing*, *21*(5), 591-595.
7. Bredas, J. L. (2014). Mind the gap!. *Materials Horizons*, *1*(1), 17-19.
8. Divya, R., Meena, M., Mahadevan, C. K., & Padma, C. M. (2014). Investigation on CuO dispersed PVA polymer films. *Journal of Engineering Research and Applications*, *4*(5), 1-7.
9. Sperling, L. H. (2015). *Introduction to physical polymer science*. John Wiley & Sons.
10. Srikanth, C., Sridhar, B. C., Prasad, M. V. N., & Mathad, R. D. (2016). Characterization and DC conductivity of novel ZnO doped polyvinyl alcohol (PVA) nano-composite films. *Journal of Advanced Physics*, *5*(2), 105-109.

11. Kidowaki, H., Oku, T., Akiyama, T., Suzuki, A., Jeyadevan, B., & Cuya, J. (2012). Fabrication and characterization of CuO-based solar cells. *Journal of Materials Science Research*, *1*(1), 138.

12. Lim, Y. F., Choi, J. J., & Hanrath, T. (2012). Facile Synthesis of Colloidal CuO Nanocrystals for Light-Harvesting Applications. *Journal of Nanomaterials*, *2012*(1), 393160.

13. Chiang, C. Y., Aroh, K., & Ehrman, S. H. (2012). Copper oxide nanoparticle made by flame spray pyrolysis for photoelectrochemical water splitting–Part I. CuO nanoparticle preparation. *International journal of hydrogen energy*, *37*(6), 4871-4879.

14. Ashokkumar, S. P., Vijeth, H., Yesappa, L., Niranjana, M., Vandana, M., & Devendrappa, H. (2020). Electrochemically synthesized polyaniline/copper oxide nano composites: To study optical band gap and electrochemical performance for energy storage devices. *Inorganic Chemistry Communications*, *115*, 107865.

15. Jundale, D. M., Navale, S. T., Khuspe, G. D., Dalavi, D. S., Patil, P. S., & Patil, V. B. (2013). Polyaniline–CuO hybrid nanocomposites: synthesis, structural, morphological, optical and electrical transport studies. *Journal of Materials Science: Materials in Electronics*, *24*, 3526-3535.

16. SINGH, S. K., Verma, A., Lakhan, R., & Shukla, R. K. (2014). Structural and optical studies of CuO doped polyaniline. *Int. J. Manage. Inform. Technol. Eng.*, *2*, 85-92.

17. Kanchana, S. K., Vanitha, N., Basavaraj, R. B., & Madivalappa, S. (2023). Structural and optical properties of polyvinyl alcohol/copper oxide (PVA/CuO) nanocomposites. *Solid State Communications*, *370*, 115221.

18. Athisayaraj, E. P. P., & Vedhi, C. (2019). Composites of copper oxide and polyaniline for solar cell applications. *n. o*, *4*.

19. Ashokkumar, S. P., Vijeth, H., Veeresh, S., Nagaraju, Y. S., Ganesh, H., Basappa, M., ... & Devendrappa, H. (2020, June). Structure, morphology and optical properties of CuO nano particles immersed PANI/Li composite. In *AIP Conference Proceedings* (Vol. 2244, No. 1). AIP Publishing.

20. Yeo, J. K., Sperling, L. H., & Thomas, D. A. (1981). Poly (n-Butyl acrylate)/polystyrene interpenetrating polymer networks and related materials. II. Aspects of molecular mixing via modulus-temperature studies. *Polymer Engineering & Science*, *21*(11), 696-702.

21. Ashokan, S., Ponnuswamy, V., & Jayamurugan, P. (2015). Synthesis and characterization of CuO nanoparticles, DBSA doped PANI and PANI/DBSA/CuO hybrid composites for diode and solar cell device development. *Journal of Alloys and Compounds*, *646*, 40-48.